

Article

Talaromarins A–F: Six New Isocoumarins from Mangrove-Derived Fungus *Talaromyces flavus* TGGP35

Jin Cai ^{1,2,†}, Xiao-Chen Zhu ^{3,†}, Wei-Nv Zeng ^{1,2}, Bin Wang ^{1,2}, You-Ping Luo ^{1,2}, Jing Liu ^{1,2}, Min-Jing Chen ^{1,2}, Gao-Yu Li ^{1,2}, Guo-Lei Huang ^{1,2}, Guang-Ying Chen ^{1,2}, Jing Xu ^{3,*} and Cai-Juan Zheng ^{1,2,*}

¹ Key Laboratory of Tropical Medicinal Resource Chemistry of Ministry of Education, College of Chemistry and Chemical Engineering, Hainan Normal University, Haikou 571158, China; caijin20210207@163.com (J.C.); z17889949296@163.com (W.-N.Z.); 15180328507@163.com (B.W.); lyp188089688692022@163.com (Y.-P.L.); liujing3182799099@163.com (J.L.); cmj19151835730@163.com (M.-J.C.); qqwbma_999@163.com (G.-Y.L.); 070333@hainnu.edu.cn (G.-L.H.); chgying@163.com (G.-Y.C.)

² Key Laboratory of Tropical Medicinal Plant Chemistry of Hainan Province, Haikou 571158, China

³ Key Laboratory of Advanced Materials of Tropical Island Resources of Ministry of Education, School of Chemical Engineering and Technology, Hainan University, Haikou 570228, China; zhuxiaochenlucky@163.com

* Correspondence: happyjing3@hainanu.edu.cn (J.X.); caijuan2002@163.com (C.-J.Z.)

† These authors contributed equally to this work.

Abstract: Six new isocoumarin derivative talaromarins A–F (1–6), along with 17 known analogues (7–23), were isolated from the mangrove-derived fungus *Talaromyces flavus* (Eurotiales: Trichocomaceae) TGGP35. Their structures were identified by detailed IR, UV, 1D/2D NMR and HR-ESI-MS spectra. The absolute configurations of new compounds were determined by the modified Mosher's method and a comparison of their CD spectra with dihydroisocoumarins described in the literature. The antioxidant, antibacterial, anti-phytopathogenic and inhibitory activity against α -glucosidase of all the isolated compounds were tested. Compounds 6–11, 17–19 and 21–22 showed similar or better antioxidant activity than the IC₅₀ values ranging from 0.009 to 0.27 mM, compared with the positive control trolox (IC₅₀ = 0.29 mM). Compounds 10, 18, 21 and 23 exhibited strong inhibitory activities against α -glucosidase with IC₅₀ values ranging from 0.10 to 0.62 mM, while the positive control acarbose had an IC₅₀ value of 0.5 mM. All compounds showed no antibacterial or anti-phytopathogenic activity at the concentrations of 50 μ g/mL and 1 mg/mL, respectively. These results indicated that isocoumarins will be useful to developing antioxidants and as diabetes control agents.

Keywords: *Talaromyces flavus*; isocoumarins; antioxidant; antibacterial; α -glucosidase inhibitory activity; anti-phytopathogenic



Citation: Cai, J.; Zhu, X.-C.; Zeng, W.-N.; Wang, B.; Luo, Y.-P.; Liu, J.; Chen, M.-J.; Li, G.-Y.; Huang, G.-L.; Chen, G.-Y.; et al. Talaromarins A–F: Six New Isocoumarins from Mangrove-Derived Fungus *Talaromyces flavus* TGGP35. *Mar. Drugs* **2022**, *20*, 361. <https://doi.org/10.3390/md20060361>

Academic Editor: Hee Jae Shin

Received: 22 April 2022

Accepted: 24 May 2022

Published: 27 May 2022

Publisher's Note: MDPI stays neutral with regard to jurisdictional claims in published maps and institutional affiliations.



Copyright: © 2022 by the authors. Licensee MDPI, Basel, Switzerland. This article is an open access article distributed under the terms and conditions of the Creative Commons Attribution (CC BY) license (<https://creativecommons.org/licenses/by/4.0/>).

1. Introduction

Marine fungi, particularly the mangrove-derived fungi, have proven to be a prolific source of structurally novel and biologically active secondary metabolites, which increasingly attracted the attention of both pharmaceutical and natural product chemists [1–3]. Up to now, more than 1400 new secondary metabolites produced by mangrove-derived fungi have been reported, including polyketides, alkaloids, terpenes and so on, and more than 40% of secondary metabolites displayed cytotoxic, antibacterial and insecticidal activities etc. [3–8]. Among them, isocoumarins are lactone-type derivatives derived from the polyketide pathway [9,10], and they possess a wide range of pharmacological activities such as antibacterial 7-hydroxyoospolactone and parapholactone [11], anti-inflammatory (\pm)-prunomarin A [12], cytotoxic lunatinin [13], insecticidal peniciisocoumarins A and B, antiplasmodial monocerin [14], antioxidant and α -glucosidase inhibitory penicimarin N [15], brine shrimp (*Artemia salina*) lethal and broad-spectrum antimicrobial penicimarin G–K [16,17], penicoffrazins B and C [18].

The genus of *Talaromyces* has been studied and applied as a biocontrol agent, as a rich source of chitinolytic enzymes and producer of secondary metabolites [19–21]. Different classes of bioactive secondary metabolites have been found from the genus of *Talaromyces* [19–21], including some bioactive isocoumarins, such as selective antimigratory talarolactone A [22], α -glucosidase inhibitory sescandelin B and 3,4-dimethyl-6,8-dihydroxyisocoumarin [23], antibacterial tratenopyrone [24], antibacteria and antifungi (-)-8-hydroxy-3-(4-hydroxypentyl)-3,4-dihydroisocoumarin [25]. These results indicated that the genus of *Talaromyces* can be used for the control of pathogenic bacteria, phytopathogenic microorganisms, diabetes control agents and so on [19,26].

As part of our continuing exploration of structurally novel and biologically interesting secondary metabolites from mangrove-derived fungi [27–33], a fungus *Talaromyces flavus* TGGP35 obtained from the medicinal mangrove plant *Acanthus ilicifolius* attracted our attention, because of the EtOAc extract of *T. flavus* TGGP35 showed potent antioxidant activity. A chemical investigation of this fungus led to the identification of six new isocoumarins talaromarin A–F (1–6) and 17 known analogues (7–23) (Figure 1). Herein, we report the isolation, structure identification, and bioactivities of these compounds.

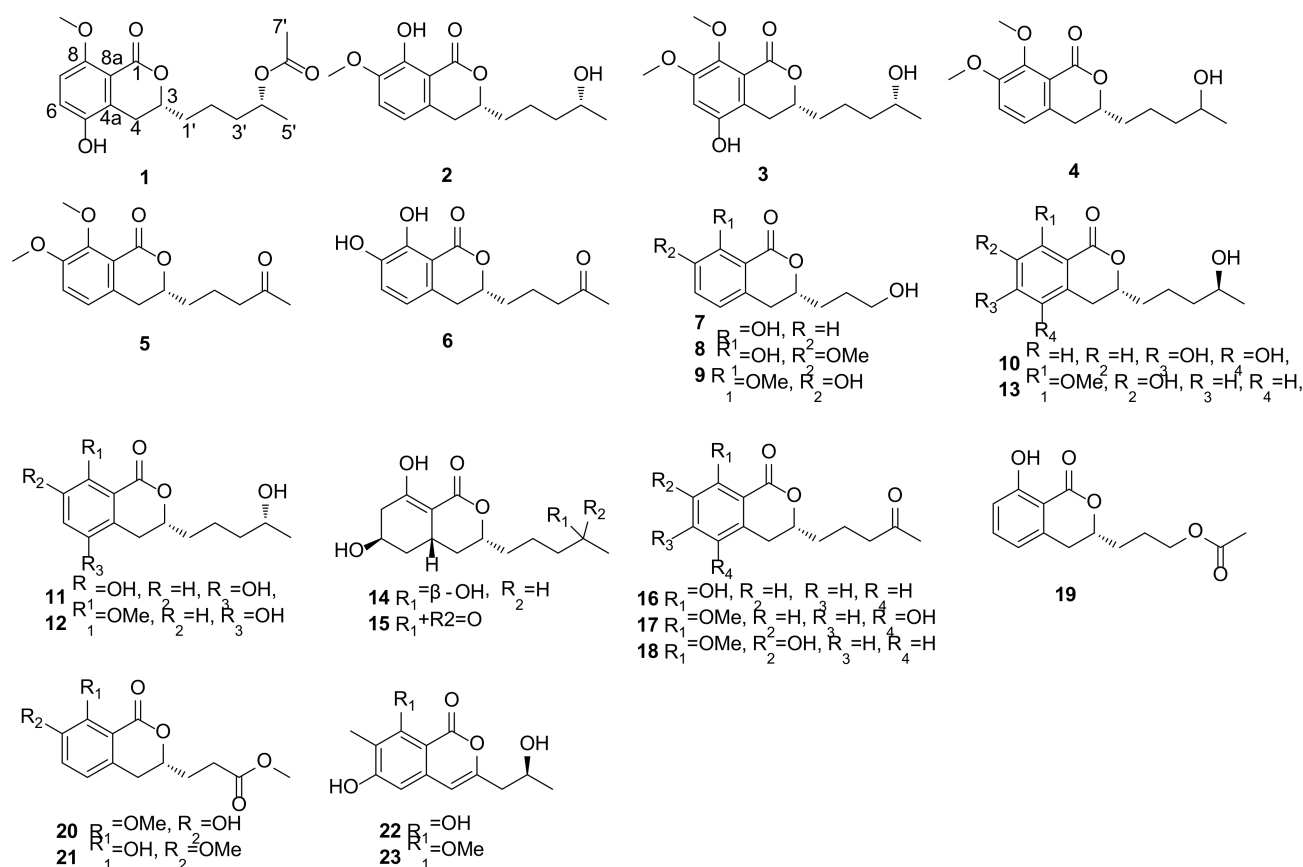


Figure 1. The structures of compounds 1–23.

2. Results and Discussion

Compound 1 was isolated as a colorless oil. The molecular formula of 1 was established as C₁₇H₂₂O₆ (seven degrees of unsaturation) by its HR-ESI-MS spectrum at m/z 323.1475 [M + H]⁺ (calcd for C₁₇H₂₃O₆, 323.1472). The IR spectrum showed the presence of a hydroxyl group (3432 cm⁻¹) and an aromatic ring (1743, 1618 and 1388 cm⁻¹) in 1. The ¹H-NMR data (Table 1) displayed a pair of ortho coupled aromatic protons at δ_H 7.00 (d, J = 8.8 Hz) and 6.78 (d, J = 8.8 Hz), one methoxyl group at δ_H 3.88 (s), two oxygenated methine groups at δ_H 4.90 (m) and 4.34 (m), four methylene groups at δ_H [3.08 (m) and 2.64 (m)], 1.85 (m), 1.57 (m) and 1.52 (m), one methyl group at δ_H 1.22 (d, J = 6.4 Hz).

The combination of ^{13}C NMR and DEPT data (Table 2) exhibited 17 carbon resonances, including two ester carbonyls at δ_{C} (171.1 and 163.1), six aromatic carbons at δ_{C} (155.5, 145.3, 128.4, 121.2, 114.6 and 111.5), one methoxyl group at δ_{C} (56.6), two oxygenated methine groups at δ_{C} (77.4 and 70.9), four methylene groups at δ_{C} (35.7, 34.7, 28.0 and 21.0), two methyl groups at δ_{C} (21.6 and 20.1). The above 1D NMR spectroscopic data indicated that **1** had an isocoumarin skeleton structure, and **1** is similar to penicimarin G (**12**) [16]. The major difference was the presence of an acetoxy group at [δ_{C} 171.1 (C), 21.6 (CH_3) and δ_{H} 2.04, (s)] in **1**, indicating that the hydroxyl group in **12** was replaced by an acetoxy group in **1**. The ^1H - ^1H COSY correlations of $\text{CH}_2(2')\text{-CH}_2(3')\text{-CH}(4')\text{-CH}_3(5')$, combined with the HMBC correlations from H-5' to C-4'/C-3' (Figure 2), confirmed the acetoxy group connected at C-4' in **1**, and the planar structure of **1** was determined (Figure 1).

Table 1. ^1H NMR spectroscopic data (400/600 MHz) (δ in ppm, J in Hz) for **1–6** in CDCl_3 .

Position	1	2	3	4	5	6
3	4.34, m	4.54, m	4.35, m	4.36, m	4.37, m	4.58, m
4	2.64, dd (16.4, 11.6) 3.08, dd (16.4, 2.8)	2.86, m	2.56, m 2.98, m	2.82, m	2.82, m	2.87, m
5		6.62, d (8.0)		6.91, d (8.0)	6.91, d (8.4)	6.61, d (8.0)
6	7.00, d (8.8)	6.98, d (8.4)	6.67, s	7.06, d (8.0)	7.06, d (8.0)	7.07, d (8.0)
7	6.78, d (8.8)					
7-OH						5.53, s
7-OMe		3.87, s	3.84, s	3.88, s	3.88, s	
8-OMe	3.88, s		3.89, s	3.96, s	3.95, s	
8-OH		11.18, s				11.00, s
1'	1.85, m	1.87, m	1.85, m	1.88, m	1.82, m	1.78, m
2'	1.57, m	1.58, m	1.60, m	1.58, m	1.78, m	1.80, m
3'	1.52, m	1.47, m	1.50, m	1.51, m	2.52, t (6.4)	2.53, m
4'	4.90, m	3.80, m	3.82, m	3.83, m		
5'	1.22, d (6.4)	1.19, d (6.4)	1.21, d (6.0)	1.21, d (4.0)	2.16, s	2.15, m
7'	2.04, s					

Table 2. ^{13}C NMR spectroscopic data (100/150 MHz) for **1–6** in CDCl_3 .

Position	1	2	3	4	5	6
1	163.1, C	170.4, C	162.7, C	162.6, C	162.5, C	170.2, C
3	77.4, CH	80.4, CH	78.3, CH	78.5, CH	78.3, CH	80.6, CH
4	28.0, CH_2	32.4, CH_2	27.4, CH_2	33.8, CH_2	33.7, CH_2	32.2, CH_2
4a	128.4, C	130.1, C	119.9, C	132.3, C	132.2, C	129.7, C
5	145.3, C	117.1, CH	147.7, CH	122.4, CH	122.4, CH	117.9, CH
6	121.2, CH	117.5, CH	106.1, C	117.5, CH	117.4, CH	120.8, CH
7	111.5, CH	147.4, C	153.1, C	153.0, C	153.0, C	143.9, C
8	155.5, C	152.5, C	142.9, C	151.6, C	151.5, C	149.1, C
8a	114.6, C	108.6, C	117.7, C	119.6, C	119.5, C	108.4, C
7-OMe		56.4, CH_3	56.6, CH_3	56.5, CH_3	56.5, CH_3	
8-OMe	56.6, CH_3		61.8, CH_3	61.7, CH_3	61.7, CH_3	
1'	34.7, CH_2	34.8, CH_2	34.9, CH_2	34.8, CH_2	34.0, CH_2	34.1, CH_2
2'	21.0, CH_2	21.3, CH_2	21.5, CH_2	21.5, CH_2	19.4, CH_2	19.2, CH_2
3'	35.7, CH_2	38.9, CH_2	39.1, CH_2	39.1, CH_2	43.2, CH_2	43.0, CH_2
4'	70.9, CH	67.9, CH	68.2, CH	68.1, CH	208.7, C	208.6, C
5'	20.1, CH_3	23.7, CH_3	23.8, CH_3	23.8, CH_3	30.1, CH_3	30.1, CH_3
6'	171.1, C					
7'	21.6, CH_3					

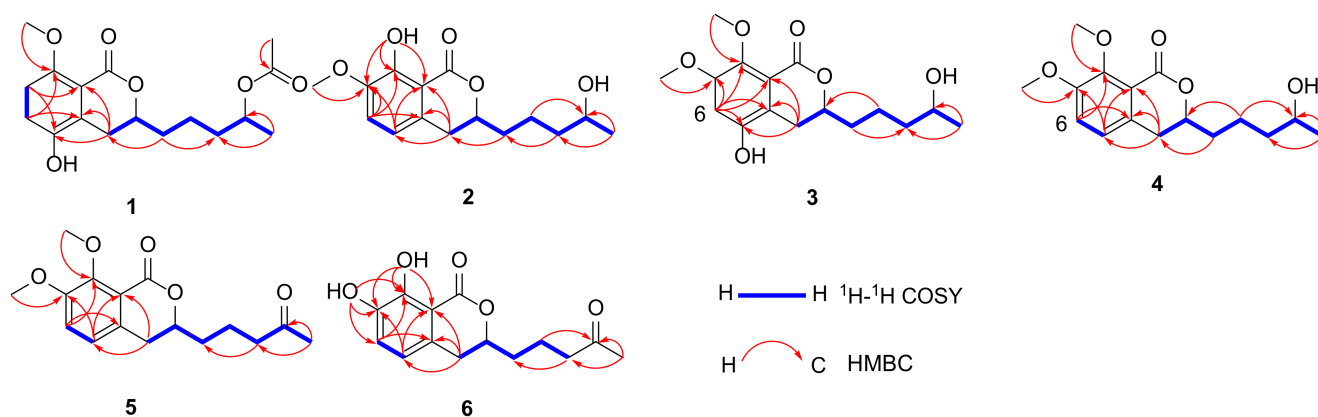


Figure 2. ^1H - ^1H COSY and key HMBC correlations for compounds 1–6.

The absolute configurations of C-3 and C-4' in **1** were determined by chemical hydrolysis, modified Mosher's method and a comparison of CD spectra with dihydroisocoumarins described in the literature [28,34]. The major hydrolysis product (**1a**) of **1** was obtained with K_2CO_3 and anhydrous ethanol at 28 °C for 1.5 h (Figure 3), and **1a** showed the same planar structure with **12** [16]. The modified Mosher's method was used to determine the configuration of C-4' for **1a**. The differences in ^1H NMR chemical shifts of **1a** between (S)- and (R)-MTPA esters ($\Delta\delta = \delta_S - \delta_R$) were calculated to assign the absolute configuration of C-4' to be R (Figure 4), the same as **12** [16]. The negative cotton effect at 266 nm suggested the R configuration at C-3 (Figure 5), by comparison with data for dihydroisocoumarins described in the literature [34]. Thus, the structure of **1** was determined and named talaromarin A.

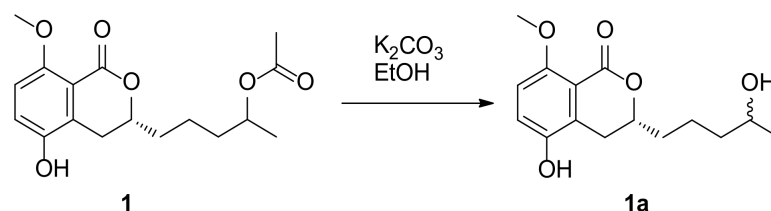


Figure 3. Reaction route of hydrolysis for compound 1.

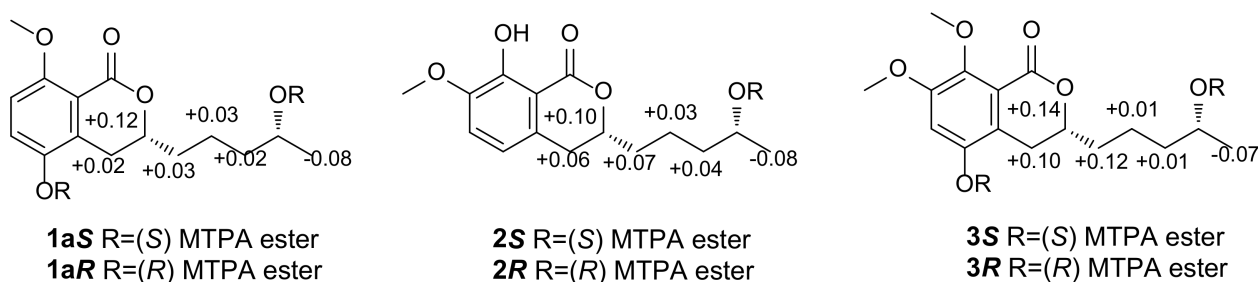


Figure 4. $\Delta\delta (= \delta_S - \delta_R)$ values for (S)- and (R)-MTPA esters of compounds 1–3.

Compound **2** was isolated as a white powder. The molecular formula was deduced to be $\text{C}_{15}\text{H}_{20}\text{O}_5$ on the basis of HR-ESI-MS spectrum, implying six degrees of unsaturation. According to the IR spectrum, the hydroxyl group (3414 cm^{-1}) and aromatic rings (1668 , 1619 , 1586 , 1502 and 1442 cm^{-1}) were observed. The ^1H and ^{13}C NMR spectroscopic data (Tables 1 and 2) revealed that **2** also belonged to the isocoumarin class and had a similar structural relationship to penicimarin M [17], except for the presence of one oxygenated methine at [δ_{H} 3.80 (m), δ_{C} 67.9 (CH)] for C-4', and the absence of a carbonyl group at δ_{C} 208.4 (C) in **2**. The above results suggested a carbonyl group in penicimarin M was

replaced by an oxygenated methine group in **2**. Furthermore, the ^1H - ^1H COSY correlations of H-5' to H-4' and H-3' to H-2'/H-4', and the HMBC correlations from the methyl H-5' to C-3'/C-4' established the oxygenated methine at C-4' (Figure 2). The absolute configuration of C-4' was determined as *R* by Mosher's method [28] (Figure 4). The negative cotton effect at 265 nm suggested the *R* configuration at C-3 (Figure 5), by comparison with data for dihydroisocoumarins described in the literature [34]. Thus, the absolute configuration of **2** was established as $3R,4'R$ and named talaromarin B.

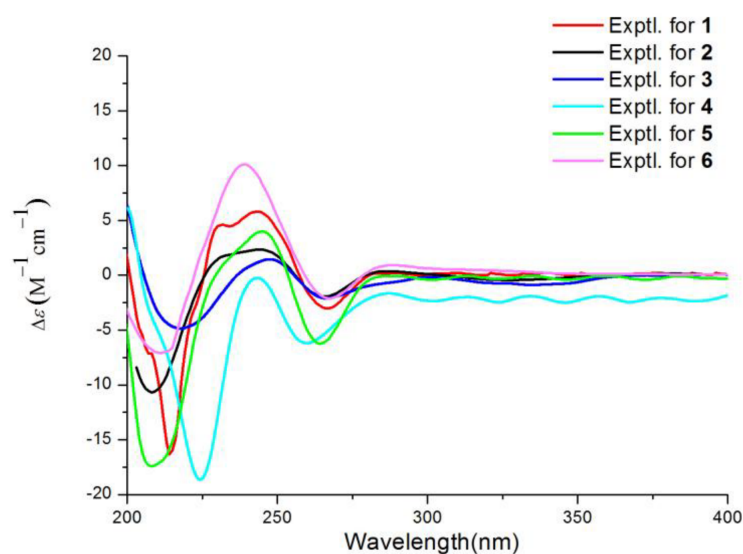


Figure 5. The experimental CD spectra of compounds 1–6.

Compound **3** was isolated as a yellow oil, with the molecular formula $\text{C}_{16}\text{H}_{22}\text{O}_6$ (six degrees of unsaturation) by the HR-ESI-MS spectrum. The IR spectrum indicated that **3** had hydroxyl group (3415 cm^{-1}) and aromatic ring (1638 , 1618 and 1384 cm^{-1}). The ^1H , ^{13}C NMR data (Tables 1 and 2) and HR-ESI-MS data revealed that **3** closely resembled those of **2**, the main differences were the presence of a methoxyl group at [δ_{H} 3.89 (s), δ_{C} 61.8 (CH_3)] in **3**, and an aromatic proton signal at δ_{H} 6.62 (d, $J = 8.0\text{ Hz}$) was absent in **3**. Moreover, the chemical shift of C-5 at δ_{C} (117.1) in **2** was downfield-shifted to δ_{C} (147.7) in **3**. The HMBC correlations from 8-OCH₃ to C-8, 7-OCH₃ to C-7 and H-6 to C-8/C-7/C-4a (Figure 2), indicated the additional methoxyl group was attached to C-8 and the hydroxyl group was connected to C-5 (Figure 2). The absolute configurations of C-3 and C-4' were determined to be the same *R* by comparison with CD data described in the literature [34] and Mosher's method [28] (Figures 4 and 5). Thus, the structure of **3** was determined and named talaromarin C.

Compound **4** was isolated as a yellow oil, and the molecular formula was established as $\text{C}_{16}\text{H}_{22}\text{O}_5$ (six degrees of unsaturation) on the basis of its HR-ESI-MS spectrum. The IR spectrum of **4** displayed absorption bands for hydroxyl (3475 cm^{-1}), carbonyl (1706 cm^{-1}) and aromatic (1637 and 1617 cm^{-1}) groups. The ^1H and ^{13}C NMR spectroscopic data (Tables 1 and 2) suggested that **4** was very similar to those of **2**, the only difference was the presence of a methoxyl group at [δ_{H} 3.96 (s) and δ_{C} 61.7 (CH_3)] in **4**. The location of the methoxyl groups at C-7 and C-8 were established by HMBC correlations from 7-OCH₃ to C-7, 8-OCH₃ to C-8, H-6 to C-8/C-4a and H-5 to C-7/C-8a/C-4 (Figure 2). The ^1H - ^1H COSY, HMQC, and HMBC spectra established the complete assignment for **4** (Figure 2). Mosher's method was tried to determine the absolute configuration of C-4' in **4** [28]; unfortunately, the reaction failed. The negative cotton effect at 259 nm suggested the *R* configuration at C-3 (Figure 5) [34]. Thus, the structure of **4** was determined and named talaromarin D.

Compound **5** was isolated as a colorless oil and had the molecular formula of $\text{C}_{16}\text{H}_{20}\text{O}_5$ as determined by HR-ESI-MS and NMR data, requiring seven degrees of unsaturation. The presence of an aromatic ring (1638 , 1617 cm^{-1}) was observed in the IR spectrum. The ^1H

and ^{13}C NMR data (Tables 1 and 2) of **5** were structurally similar to those of **4**, except for the presence of a ketone carbonyl carbon at δ_{C} 208.7 (C) and the absence of one oxygenated methine carbon at [δ_{C} 68.1 (CH), δ_{H} 3.83 (m)] at C-4' in **5**, indicating that the oxygenated methine group in **4** was replaced by a carbonyl group for C-4' in **5**. The HMBC correlations from H-3' to C-1', H-5' to C-4'/C-3' further confirmed **5** with a carbonyl unit at C-4' (Figure 2). The whole structure was further determined by the 2D NMR spectra (Figure 2). The absolute configuration of C-3 was determined as *R* by CD spectra (Figure 5) [34], and **5** was named talaromarin E.

Compound **6** was isolated as a yellow oil. The molecular formula of **6** was established as $\text{C}_{14}\text{H}_{16}\text{O}_5$ (seven degrees of unsaturation) on the basis of its HR-ESI-MS data. The IR spectrum of **6** showed the hydroxyl group at 3461 and 3407 cm^{-1} and the aromatic rings at 1736 and 1671 cm^{-1} . The ^1H and ^{13}C NMR spectroscopic data (Tables 1 and 2) revealed that **6** was an isocoumarin derivative, with a similar structural relationship to peniciisocoumarin D (**18**), the obvious difference was that **6** lacked a methoxy group at C-8. The methoxy group (8-OMe) in **18** was replaced by a hydroxy group (8-OH) in **6**, which was supported by the appearance of a hydrogen-bonded hydroxyl group at δ_{H} 11.00 (s). The HMBC correlations from the hydroxyl group 8-OH to C-8a/C-8/C-7 further confirmed the 8-OH was connected at C-8 (δ_{C} 149.1) (Figure 2). The ^1H - ^1H COSY, HMQC, and HMBC spectra determined the complete assignment for **6** (Figure 2). The absolute configuration of C-3 was determined as *R* by CD spectroscopy (Figure 5) [34] and **6** was named talaromarin F.

By comparing physical and spectroscopic data with the literature, the 17 known homologues were identified as (*R*)-3-(3-hydroxypropyl)-8-hydroxy-3,4-dihydroisocoumarin (**7**) [35], peniciisocoumarin C (**8**) [28], 7-hydroxy-3-(3-hydroxypropyl)-8-methoxyisochroman-1-one (**9**) [34], 5,6-dihydroxy-3-(4-hydroxypentyl)-isochroman-1-one (**10**) [23], peniciisocoumarin F (**11**) [28], penicimarins G (**12**) [16], penicimarins C (**13**) [36], peniciisocoumarin A (**14**) [28], peniciisocoumarin B (**15**) [28], aspergillumarin A (**16**) [37], penicimarins H (**17**) [16], peniciisocoumarin D (**18**) [28], peniciisocoumarin G (**19**) [28], peniciisocoumarin E (**20**) [28], penicimarins N (**21**) [15], 6,8-dihydroxy-3-(2-hydroxypropyl)-7-methyl-1*H*-isochroman-1-one (**22**) [38] and pestalotiorin (**23**) [39].

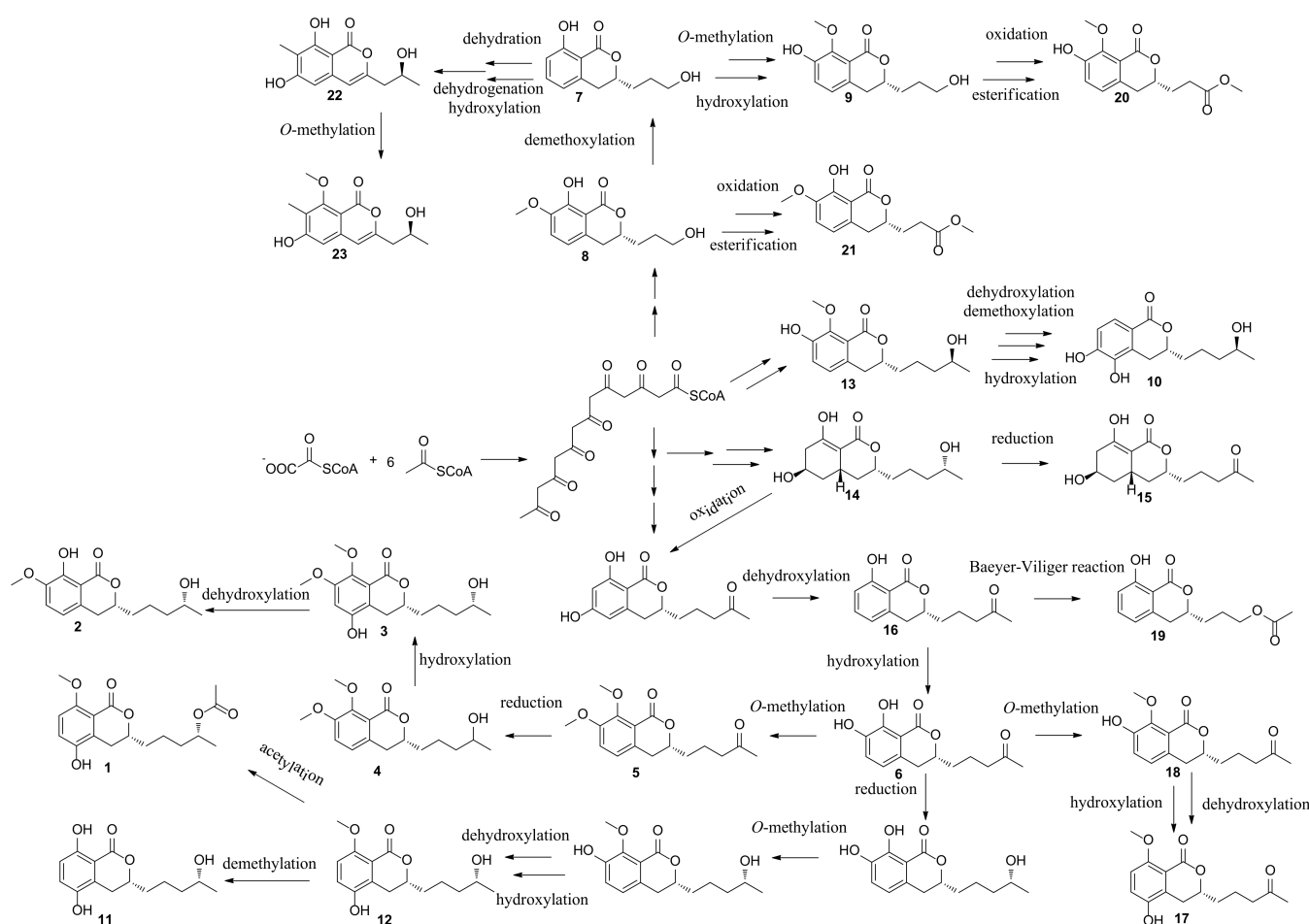
The plausible biosynthetic pathways of compounds **1–23** were also proposed (Scheme 1). Isocoumarins were originated from the acetate-malonate or the polyketide synthase (PKS) pathway [10]. Peniciisocoumarin C (**8**), penicimarins C (**13**) and peniciisocoumarin A (**14**) would be biosynthesized from malonyl-CoA and acetyl-CoA and can be considered as intermediates which would be transformed to other isolated compounds from the fungus TGGP35. Compound **8** would be transformed to **7**, **9** and **20–23** by condensation, aromatization, esterification, dihydroxylation, methoxylation reaction and so on. Compound **13** would be transformed to **10** by dehydroxylation, demethoxylation and dehydroxylation reaction. Compounds **1–6**, **10–15** and **17–19** would be deduced from **14** with dihydroxylation, methoxylation, methylation, hydroxylation, esterification, acetylation, Baeyer–Viliger oxidation reaction, etc.

The antioxidant activities of compounds **1–23** were evaluated. Compounds **6–11**, **17–19** and **22** exhibited potent antioxidant activity with the IC_{50} values ranging from 0.009 to 0.27 mM, while the positive control trolox was $\text{IC}_{50} = 0.29$ mM (Table 3).

Table 3. Antioxidant activity for compounds **2**, **6–11**, **17–19**, **21** and **22**.

Compound	2	6	7	8	9	10	11	17	18	19	21	22	Trolox ^a
IC_{50} (mM)	28.39	0.14	0.17	0.13	0.10	0.11	0.12	0.12	0.16	0.15	20.66	0.009	0.29

^a Trolox was used as a positive control.



Scheme 1. Plausible biosynthetic pathways of compounds 1–23.

The preliminary structure–activity relationship of the isolated isocoumarins was discussed. The substitution site, orientation of hydroxyl and methoxy groups on the skeleton of isocoumarins, and the substitution of different groups by side chain C-4' can affect their antioxidant activity. Compound 2 which possesses a hydroxyl group on C-8, showed better antioxidant activity than that of 3 and 4, indicating that the chelated hydroxyl group at C-8 is important in enhancing antioxidant activity. Compound 6 possesses two hydroxyl groups at C-7 and C-8, which showed higher antioxidant activity than 16 (only one hydroxyl group on C-8), indicating that the hydroxyl group at C-7 is an important antioxidant activity site. Compounds 17 and 18 possess a ketone group at C-4', which showed higher antioxidant activity than 12 and 13, which have an oxygenated methine at C-4', suggesting that the substitution of different groups by side chain at C-4' can affect antioxidant activity. Compound 22 possesses a hydroxyl group at C-8, showed higher antioxidant activity than 23, suggesting that the chelated hydroxyl group at C-8 is important in enhancing antioxidant activity. Furthermore, compounds 7, 8, 19 and 21 show antioxidant activities, which may be due to the existence of a chelated hydroxyl group.

Compounds 10, 18, 21, and 23 showed strong inhibitory activity against α -glucosidase with the IC_{50} values of 0.10, 0.38, 0.62 and 0.54 mM, respectively (the positive control acarbose with the IC_{50} value of 0.5 mM).

All compounds were tested for their antibacterial activities against *Staphylococcus aureus*, *Escherichia coli*, *S. epidermidis* and *Pseudomonas aeruginosa*; however, all compounds showed no antibacterial activity at the concentration of 50 μ g/mL. All compounds showed no biological activity against five phytopathogens (*Colletotrichum asianum*, *C. acutatum*,

Fusarium oxysporum, *Pyricularia oryzae* and *Curvularia australiensis*) at the concentration of 1 mg/mL.

3. Materials and Methods

3.1. General Experimental Procedures

Optical rotations were measured on a JASCO P-1020 digital polarimeter (JASCO, Tokyo, Japan). IR spectra were recorded on a Thermo Nicolet 6700 (using KBr disks) spectrophotometer. UV spectra were measured on a PERSEE TU-1990 spectrophotometer. CD spectra were recorded on a Mos-450 spectrometer and 1D and 2D NMR spectra were recorded on a Bruker AV spectrometer (400 MHz for ^1H and 100 MHz for ^{13}C) and a JNM-ECZS spectrometer (600 MHz for ^1H and 125 MHz for ^{13}C). HR-ESI-MS spectra were obtained on a Q-TOF Ultima Global GAA076 LC mass spectrometer. ESI-MS spectra were recorded on a MAT-95-MS mass spectrometer. HPLC were used for the Agilent 1100 prep-HPLC system with an Agilent C18 analytical (9.4 × 250 mm, 5 μm) HPLC column. Silical gel (200–300 mesh, Qingdao Marine Chemical Factory, Qingdao, China) were used for column chromatography (CC). Sephadex LH-20 gel column (GE Healthcare, Bio-Sciences Corp, Piscataway, NJ, USA) were used for CC. Biological activities were tested on an ultra-clean workbench (Suzhou Sujing Company, Suzhou, China) and the biological activities' results were tested with a full wavelength multifunctional microplate reader (Bio-Tek Instruments, Winooski, VT, USA). Methanol, ethyl acetate, petroleum ether, chloroform, dimethyl sulfoxide and other conventional chemical reagents were used in the experimental operation (Guangzhou Xilong Chemical Reagent Factory, Guangzhou, China).

3.2. Fungal Materials

The fungus TGGP35 was isolated from the stem of the mangrove plant *Acanthus ilicifolius*, which were collected in the Dongzhai Port, Haikou, Hainan Province in August, 2015. The fungus was identified according to its morphological characteristics and a molecular biological protocol by 18S rRNA amplification and sequencing of the ITS region. The sequence data have been submitted to GeneBank, with accession number MT071116, and the fungal strain was identified as *Talaromyces flavus* (Eurotiales: Trichocomaceae). The strains have been stored in the Key Laboratory of Tropical Medicinal Resources Chemistry of the Ministry of Education, School of Chemistry and Chemical Engineering, Hainan Normal University (PDA medium, stored at 4 °C).

3.3. Fermentation, Extraction and Isolation

The seed culture was prepared in potato liquid medium (6 g sea salt and 10 g peptone in 2 L of potato infusion, in 1 L × 4 erlenmeyer flasks each containing 500 mL seed medium), and incubated on a rotary shaker (170 rpm) for 4 days at 28 °C. In total, 20 mL seed culture was then transferred into 1 L erlenmeyer flasks with solid rice medium with a total of 100 bottles of fermentation (each flask contained 60 mL rice, 0.6 g sea salt and 1.0 g peptone) at 28 °C for 4 weeks. The whole rice fermented material was extracted three times with EtOAc, and then concentrated in vacuo to yield crude extracts (120.8 g). The total crude extracts were subjected to silica gel column chromatography (CC) eluted with petroleum ether/EtOAc (*v/v*, gradient 100:0–0:100) and EtOAc/MeOH (*v/v*, gradient 100:0–70:30) to generate fifteen fractions (Fr. A–Fr. L). Fr. F (20.5 g) was fractionated by silica gel CC (200–300 mesh) using a gradient elution of petroleum ether/EtOAc system (7:1–0:1) to obtain ten fractions (Fr. F1–Fr. F10) by the TLC analysis. Fr. F2 (10.3 g) was subjected to Sephadex LH-20 (Petroleum ether–CHCl₃–MeOH, 2:1:1, *v/v*), and then to semi-preparative HPLC (MeOH–H₂O, 70:30, *v/v*) to give compounds **1** (4.2 mg), **2** (5.5 mg), **3** (3.8 mg), **5** (4.5 mg) and **7** (4.7 mg). Subfraction Fr. F3 was further separated by semi-preparative HPLC (MeOH–H₂O, 60:40, *v/v*) for four subfractions Fr. F3a–3d. Compounds **6** (4.7 mg), **8** (5.5 mg), **9** (5.8 mg), and **10** (3.5 mg) were isolated from subfraction Fr. F3a. Compounds **11** (3.7 mg), **14** (4.7 mg), **16** (5.5 mg), **17** (5.8 mg) and **19** (3.5 mg) for subfraction Fr. F3b. Compounds **12** (6.3 mg), **13** (3.2 mg) and **15** (5.7 mg) for subfraction Fr. F3c, and compounds

18 (6.8 mg), **19** (6.2 mg) and **21** (3.6 mg) for subfraction Fr. F3d. Fr. F4 (5.4 g) were subjected to Sephadex LH-20 (CHCl₃-MeOH, 1:1, *v/v*), then used for semi-preparative HPLC (MeOH-H₂O, 65:35, *v/v*) to give compound **20** (3.0 mg). Fr. F5 (2.4 g) was subjected to Sephadex LH-20 (CHCl₃-MeOH, 1:1, *v/v*), then used for semi-preparative HPLC (MeOH-H₂O, 35:65, *v/v*) to give compounds **22** (3.4 mg) and **23** (2.7 mg).

Talaromarin A (1): yellow oil; $[\alpha]_D^{25}$ -21.4 (*c* 0.10, MeOH); UV (MeOH) λ_{\max} (log ϵ) 330, 221 nm; IR (KBr) ν_{\max} 3432, 1716, 1618, 1383 cm⁻¹; CD (*c* 0.05, MeOH) λ_{\max} ($\Delta\epsilon$) 243 (+5.68), 266 (-2.89) nm; ¹H and ¹³C NMR data see Tables 1 and 2; HR-ESI-MS *m/z*: 323.1475 [M + H]⁺, (C₁₇H₂₃O₆, calcd. for 323.1472).

Talaromarin B (2): white powder; $[\alpha]_D^{25}$ -23.6 (*c* 0.10, MeOH); UV (MeOH) λ_{\max} (log ϵ) 330, 255, 223 nm; IR (KBr) ν_{\max} 3414, 1668, 1619, 1586, 1502, 1442 cm⁻¹; CD (*c* 0.05, MeOH) λ_{\max} ($\Delta\epsilon$) 244 (+2.27), 265 (-2.17) nm; ¹H and ¹³C NMR data see Tables 1 and 2; HR-ESI-MS *m/z*: 279.1240 [M - H]⁻, (C₁₅H₁₉O₅, calcd. for 279.1239).

Talaromarin C (3): yellow oil; $[\alpha]_D^{25}$ -22.0 (*c* 0.10, MeOH); UV (MeOH) λ_{\max} (log ϵ) 317, 215 nm; IR (KBr) ν_{\max} 3415, 1638, 1618, 1384 cm⁻¹; CD (*c* 0.05, MeOH) λ_{\max} ($\Delta\epsilon$) 248 (+1.36), 266 (-2.01) nm; ¹H and ¹³C NMR data see Tables 1 and 2; HR-ESI-MS *m/z*: 311.1485 [M + H]⁺, (C₁₆H₂₃O₆, calcd. for 311.1482).

Talaromarin D (4): yellow oil; $[\alpha]_D^{25}$ -21.8 (*c* 0.10, MeOH); UV (MeOH) λ_{\max} (log ϵ) 313, 222 nm; IR (KBr) ν_{\max} 3475, 1706, 1637, 1617 cm⁻¹; CD (*c* 0.05, MeOH) λ_{\max} ($\Delta\epsilon$) 243 (-0.31), 259 (-6.25) nm; ¹H and ¹³C NMR data see Tables 1 and 2; HR-ESI-MS *m/z*: 295.1527 [M + H]⁺, (C₁₆H₂₃O₅, calcd. for 295.1524).

Talaromarin E (5): colorless oil; $[\alpha]_D^{25}$ -24.4 (*c* 0.10, MeOH); UV (MeOH) λ_{\max} (log ϵ) 314, 219 nm; IR (KBr) ν_{\max} 1638, 1617 cm⁻¹; CD (*c* 0.05, MeOH) λ_{\max} ($\Delta\epsilon$) 245 (+3.93), 264 (-11.89) nm; ¹H and ¹³C NMR data see Tables 1 and 2; HR-ESI-MS *m/z*: 293.1370 [M + H]⁺, (C₁₆H₂₁O₅, calcd. for 293.1374).

Talaromarin F (6): yellow oil; $[\alpha]_D^{25}$ -21.2 (*c* 0.10, MeOH); UV (MeOH) λ_{\max} (log ϵ) 328, 254, 223 nm; IR (KBr) ν_{\max} 3481, 3407, 1736, 1671 cm⁻¹; CD (*c* 0.05, MeOH) λ_{\max} ($\Delta\epsilon$) 238 (+10.12), 267 (-2.07) nm; ¹H and ¹³C NMR data see Tables 1 and 2; HR-ESI-MS *m/z*: 265.1050 [M + H]⁺, (C₁₄H₁₇O₅, calcd. for 265.1053).

3.4. Preparations of the (S)- and (R)-MTPA Esters of Compounds 1, 2 and 3

Compound **1** was hydrolyzed in anhydrous ethanol solution for 90 min with potassium carbonate in an equivalent ratio of 1:2; the mixed product after hydrolysis was purified by semi-preparative HPLC (MeOH-H₂O, 70:30, *v/v*) to obtain **1a**. The preparation of (S)- and (R)-MTPA ester derivatives of **1a**, **2** and **3** was performed as described previously [28].

Hydrolysate of **1 (1a)**: ¹H NMR (CDCl₃, 400 MHz): δ_H 6.99 (1H, d, *J* = 8.8 Hz, H-6), 6.79 (1H, d, *J* = 8.8 Hz, H-7), 4.26 (1H, m, H-3), 3.83 (1H, m, H-4'), 3.10 and 2.63 (2H, m, H-4), 1.90 (2H, m, H-1'), 1.70 (2H, m, H-2'), 1.50 (2H, m, H-3'), 1.21 (3H, d, *J* = 6.0 Hz, H-5'); ¹³C NMR (CDCl₃, 100 MHz): δ_C 163.3, 159.4, 151.5, 145.1, 135.0, 128.5, 121.2, 111.4, 68.2, 56.6, 39.1, 34.9, 28.0, 23.8, 21.4; ESI-MS *m/z* 281.1 [M + H]⁺.

(S)-MTPA ester of **1a**: ¹H NMR (CDCl₃, 600 MHz): δ_H 7.29 (1H, d, *J* = 9.0 Hz, H-6), 6.94 (1H, d, *J* = 9.0 Hz, H-7), 5.12 (1H, m, H-4'), 4.21 (1H, m, H-3), 2.64 and 2.49 (2H, m, H-4), 1.86 (2H, m, H-1'), 1.67 (2H, m, H-2'), 1.55 (2H, m, H-3'), 1.25 (3H, d, *J* = 6.6 Hz, H-5'); ESI-MS *m/z* 758.2 [M + Na]⁺.

(R)-MTPA ester of **1a**: ¹H NMR (CDCl₃, 600 MHz): δ_H 7.31 (1H, d, *J* = 9.0 Hz, H-6), 6.94 (1H, d, *J* = 9.0 Hz, H-7), 5.11 (1H, m, H-4'), 4.09 (1H, m, H-3), 2.62 and 2.41 (2H, m, H-4), 1.83 (2H, m, H-1'), 1.64 (2H, m, H-2'), 1.53 (2H, m, H-3'), 1.33 (3H, d, *J* = 6.0 Hz, H-5'); ESI-MS *m/z* 758.2 [M + Na]⁺.

(S)-MTPA ester of **2**: ¹H NMR (CDCl₃, 600 MHz): δ_H 7.01 (1H, d, *J* = 7.8 Hz, H-5), 6.63 (1H, d, *J* = 7.8 Hz, H-6), 5.17 (1H, m, H-4'), 4.52 (1H, m, H-3), 2.82 (2H, m, H-4), 1.88 (2H, m, H-1'), 1.62 (2H, m, H-2'), 1.50 (2H, m, H-3'), 1.29 (3H, d, *J* = 6.0 Hz, H-5'); ESI-MS *m/z* 758.3 [M + Na]⁺.

(R)-MTPA ester of **2**: ¹H NMR (CDCl₃, 600 MHz): δ_H 7.01 (1H, d, *J* = 8.4 Hz, H-5), 6.62 (1H, d, *J* = 8.4 Hz, H-6), 5.16 (1H, m, H-4'), 4.42 (1H, m, H-3), 2.76 (2H, m, H-4), 1.81 (2H, m,

H-1'), 1.59 (2H, m, H-2'), 1.46 (2H, m, H-3'), 1.37 (3H, d, $J = 6.0$ Hz, H-5'); ESI-MS m/z 774.3 [M + K]⁺.

(S)-MTPA ester of 3: ¹H NMR (CDCl₃, 600 MHz): δ_{H} 6.88 (1H, s, H-6), 5.14 (1H, m, H-4'), 4.21 (1H, m, H-3), 2.43 (2H, m, H-4), 1.72 (2H, m, H-1'), 1.52 (2H, m, H-2'), 1.43 (2H, m, H-3'), 1.35 (3H, d, $J = 9.4$ Hz, H-5'); ESI-MS m/z 766.6 [M + Na]⁺.

(R)-MTPA ester of 3: ¹H NMR (CDCl₃, 600 MHz): δ_{H} 6.86 (1H, s, H-6), 5.13 (1H, m, H-4'), 4.07 (1H, m, H-3), 2.33 (2H, m, H-4), 1.65 (2H, m, H-1'), 1.51 (2H, m, H-2'), 1.42 (2H, m, H-3'), 1.28 (3H, d, $J = 9.4$ Hz, H-5'); ESI-MS m/z 766.0 [M + Na]⁺.

3.5. Biological Assays

3.5.1. Antioxidant Activity

The antioxidant activity assay was based on the reported methods [15]. The assay was performed on a 96-well microplate, the reaction was initiated by adding 10 μL of sample solution to 200 μL of ABTS working solution. All test group gradients (including positive control) were of 2.0, 1.0, 0.5, 0.25 mg/mL, respectively. PBS buffer was used as the blank control, DMSO as the negative control, and trolox as the positive control ($\text{IC}_{50} = 0.29$ mM). The antioxidant effect was evaluated by a full wavelength multifunctional microplate reader measurement at 734 nm. The inhibition rate of each sample was calculated according to the following formula: inhibition rate = $[(A_{\text{blank}} - A_{\text{compound}})/A_{\text{blank}}] \times 100\%$. Finally, the SPSS software was used to calculate the IC_{50} value.

3.5.2. Antibacterial Activity

All compounds were determined against four pathogenic bacteria: *Staphylococcus aureus* (ATCC 25923), *Escherichia coli* (ATCC 25922), *S. epidermidis* (ATCC 17749) and *Pseudomonas aeruginosa* (ATCC 17749). The concentration value of the test group and positive control was 1mg/mL by the microplate assay method [28]. The antibacterial effect was evaluated by a full wavelength multifunctional microplate reader measurement at 630 nm; the broth medium containing pathogenic bacteria was used as the blank group and DMSO as the negative control, ciprofloxacin was used as the positive control. The positive control ciprofloxacin showed antibacterial activities against four pathogenic bacteria *S. aureus*, *E. coil*, *S. epidermidis* and *P. aeruginosa* with the MIC values of 0.097, 0.78, 0.195 and 0.78 $\mu\text{g}/\text{mL}$, respectively.

3.5.3. Anti-Phytopathogenic Activity

All compounds were tested against five plant pathogens (*Colletotrichum asianum*, *C. acutatum*, *Fusarium oxysporum*, *Pyricularia oryzae* and *Curvularia australiensis*) by disk method [40]. DMSO was used as a negative control, carbendazim as a positive control. The concentration values of all test groups, negative control and positive control were 1 mg/mL; the anti-phytopathogenic results were recorded on a vernier caliper.

3.5.4. Inhibitory Activity against α -Glucosidase

The α -glucosidase inhibitory activity of the tested compounds was determined using the method in [17], with modifications for carrying it out in 96-well plates. The initial concentration of all test samples (including positive control and negative control) was 1 mg/mL, the optimized method was a mixture of 0.1 mM potassium phosphate buffer (pH = 6.8, 0.5 mL) and 10 mg/L α -glucosidase (100 μL), the testing sample (0.5 mL) was incubated at 37 °C for 5 min, and the 2.5 mM (4-nitrophenyl- β -D-glucopyranoside) PNPG (0.5 mL) was added, followed by mixing. The reaction was carried out at 37 °C for 15 min and then stopped by adding 0.2 M solution of Na₂CO₃ (0.75 mL). The inhibitory activity against α -Glucosidase was evaluated by a full wavelength multifunctional microplate reader measurement at 405 nm. Finally, inhibition rate = $[(A_{\text{control}} - A_{\text{compound}})/A_{\text{control}}] \times 100\%$. The SPSS software was used to calculate the IC_{50} value. DMSO was used as the negative control and acarbose was used as the positive control ($\text{IC}_{50} = 0.5$ mM).

4. Conclusions

In summary, 23 secondary metabolites, including six new isocoumarin derivative talaromarins A-F (1–6) and 17 known analogues (7–23) were obtained from the mangrove-derived fungus *Talaromyces flavus* TGGP35. Compounds 6–11, 17–19 and 22 exerted similar or better antioxidant activity than the positive control trolox ($IC_{50} = 0.29$ mM), with IC_{50} values ranging from 0.009 to 0.27 mM. Compounds 10, 18, 21 and 23 exhibited strong inhibitory activities against α -glucosidase with IC_{50} values ranging from 0.10 to 0.62 mM, while the IC_{50} value of positive control acarbose was 0.5 mM. All compounds showed no antibacterial or anti-phytopathogenic activity at the concentrations of 50 μ g/mL and 1 mg/mL, respectively. Their plausible biosynthetic pathway and structure–activity relationships were also explored. Therefore, these findings demonstrate the potential of these active compounds as lead compounds for developing antioxidants and as diabetes control agents.

Supplementary Materials: The following supporting information can be downloaded at: <https://www.mdpi.com/article/10.3390/md20060361/s1>, D, 2D NMR and MS data of new compounds 1–6.

Author Contributions: J.C. and X.-C.Z. performed the experiments for the isolation, structure elucidation and prepared the manuscript; W.-N.Z. and B.W. contributed to the antioxidant activity and antimicrobial evaluation; Y.-P.L. contributed to part of the structure determination; J.L., M.-J.C. and G.-Y.L. organized documents and performed basic experiments; G.-L.H. and G.-Y.C. contributed the optimization of fermentation; C.-J.Z. and J.X. supervised the research work and revised the manuscript. All authors have read and agreed to the published version of the manuscript.

Funding: This work was supported by Key Science and Technology Program of Hainan Province (No. ZDKJ202008), the National Natural Science Foundation of China (Nos. 32160108, 41866005, 82160675 and 81973229), Key Research and Development Program of Hainan Province (No. ZDYF2021SHFZ270 and ZDYF2021SHFZ108), Hainan Provincial Natural Science Foundation of China (No. 220RC593), the Innovation Platform for Academicians of Hainan Province Specific Research Fund of The Innovation Platform for Academicians of Hainan Province (No. YSPTZX202030).

Institutional Review Board Statement: Not applicable.

Informed Consent Statement: Not applicable.

Data Availability Statement: The data presented in this study are available in this article and Supplementary Material.

Conflicts of Interest: The authors declare no competing financial interest.

References

1. Carroll, A.R.; Copp, B.R.; Davis, R.A.; Keyzers, R.A.; Prinsep, M.R. Marine natural products. *Nat. Prod. Rep.* **2022**, *18*, 1R–49R. [[CrossRef](#)] [[PubMed](#)]
2. Xu, W.F.; Wu, N.N.; Wu, Y.W.; Qi, Y.X.; Wei, M.Y.; Pineda, L.M.; Ng, M.G.; Spadafora, C.; Zheng, J.Y.; Lu, L.; et al. Structure modification, antialgal, antiplasmodial, and toxic evaluations of a series of new marine-derived 14-membered resorcylic acid lactone derivatives. *Mar. Life Sci. Technol.* **2022**, *4*, 88–97. [[CrossRef](#)]
3. Chen, S.H.; Cai, R.L.; Liu, Z.M.; Gui, H.; She, Z.G. Secondary metabolites from mangrove-associated fungi: Source, chemistry and bioactivities. *Nat. Prod. Rep.* **2022**, *39*, 560–595. [[CrossRef](#)] [[PubMed](#)]
4. Jiang, H.M.; Cai, R.L.; Zang, Z.M.; Yang, W.C.; Wang, B.; Zhu, G.; Yuan, J.; She, Z.G. Azaphilone derivatives with anti-inflammatory activity from the mangrove endophytic fungus *Penicillium sclerotiorum* ZJHJJ-18. *Bioorg. Chem.* **2022**, *122*, 105721. [[CrossRef](#)]
5. Wu, Q.; Chang, Y.M.; Che, Q.; Li, D.H.; Zhang, G.J.; Zhu, T.J. Citreobenzofurans D-F and phomenones A-B: Five novel sesquiterpenoids from the mangrove-derived fungus *Penicillium* sp. HDN13-494. *Mar. Drugs* **2022**, *20*, 137. [[CrossRef](#)]
6. Qin, X.Y.; Huang, J.G.; Zhou, D.X.; Zhang, W.X.; Zhang, Y.J.; Li, J.; Yang, R.Y.; Huang, X.S. Polyketide derivatives, guhyoxyylonols A-D from a mangrove endophytic fungus *Aspergillus* sp. GXNU-Y45 that inhibit nitric oxide production. *Mar. Drugs* **2022**, *20*, 5. [[CrossRef](#)]
7. Su, J.H.; Wang, M.Q.; Li, Y.Z.; Lin, Y.S.; Gu, J.Y.; Zhu, L.P.; Yang, W.Q.; Jiang, S.Q.; Zhao, Z.X.; Sun, Z.H. Rare cytochalasans isolated from the mangrove endophytic fungus *Xylaria arbuscular*. *Fitoterapia* **2022**, *157*, 105124. [[CrossRef](#)]
8. Zeng, W.N.; Huang, G.L.; Cai, J.; Zheng, C.J. Secondary metabolites and bioactivities of *Penicillium* sp. sourced from mangrove from 2007 to 2020. *Chin. J. Org. Chem.* **2021**, *41*, 4255–4278. [[CrossRef](#)]

9. Saeed, A. Isocoumarins, miraculous natural products blessed with diverse pharmacological activities. *Eur. J. Med. Chem.* **2016**, *116*, 290–317. [[CrossRef](#)]
10. Noor, A.O.; Almasri, D.M.; Bagalagel, A.A.; Abdallah, H.M.; Mohamed, S.G.A.; Mohamed, G.A.; Ibrahim, S.R.M. Naturally occurring isocoumarins derivatives from endophytic fungi: Sources, isolation, structural characterization, biosynthesis, and biological activities. *Molecules* **2020**, *25*, 395. [[CrossRef](#)]
11. Xu, X.L.; Li, J.P.; Zhang, K.; Wei, S.Z.; Lin, R.; Polyak, S.W.; Yang, N.; Song, F.H. New isocoumarin analogues from the marine-derived fungus *Paraphoma* sp. CUGBMF180003. *Mar. Drugs* **2021**, *19*, 313. [[CrossRef](#)] [[PubMed](#)]
12. Zhang, X.Q.; Lu, Z.H.; Xia, G.R.; Song, W.M.; Guo, Z.Y.; Proksch, P. (+)-/(-)-Prunomarin A and (+)-pestalactone B, three new isocoumarin derivatives from the endophytic fungus *Phomopsis prunorum*. *Tetrahedron. Lett.* **2021**, *75*, 153205. [[CrossRef](#)]
13. Ran, Y.Q.; Lan, W.J.; Qiu, Y.; Guo, Q.; Feng, G.K.; Deng, R.; Zhu, X.F.; Li, H.J.; Dong, J. Monarubins A-C from the marine shellfish-associated fungus *Monascus ruber* BB5. *Mar. Drugs* **2020**, *18*, 100. [[CrossRef](#)] [[PubMed](#)]
14. Coronado, L.; Zhang, X.Q.; Dorta, D.; Escala, N.; Pineda, L.M.; Ng, M.G.; Olmo, E.D.; Wang, C.Y.; Gu, Y.C.; Shao, C.L.; et al. Semisynthesis, antiplasmodial activity, and mechanism of action studies of isocoumarin derivatives. *J. Nat. Prod.* **2021**, *84*, 1434–1441. [[CrossRef](#)] [[PubMed](#)]
15. Zeng, W.N.; Cai, J.; Wang, B.; Chen, L.Y.; Pan, C.X.; Chen, S.J.; Huang, G.L.; Zheng, C.J. A new bioactive isocoumarin from the mangrove-derived fungus *Penicillium* sp. TGM112. *J. Asian Nat. Prod. Res.* **2021**, 1–6. [[CrossRef](#)]
16. Huang, G.L.; Zhou, X.M.; Bai, M.; Liu, Y.X.; Zhao, Y.L.; Luo, Y.P.; Niu, Y.Y.; Zheng, C.J.; Chen, G.Y. Dihydroisocoumarins from the mangrove-derived fungus *Penicillium citrinum*. *Mar. Drugs* **2016**, *14*, 177. [[CrossRef](#)]
17. Mei, R.Q.; Wang, B.; Zeng, W.N.; Huang, G.L.; Chen, G.Y.; Zheng, C.J. Bioactive isocoumarins isolated from a mangrove-derived fungus *Penicillium* sp. MGP11. *Nat. Prod. Res.* **2022**, *36*, 1260–1265. [[CrossRef](#)]
18. Cao, J.; Li, X.M.; Li, X.; Li, H.L.; Meng, L.H.; Wang, B.G. New lactone and isocoumarin derivatives from the marine mangrove-derived endophytic fungus *Penicillium coffeae* MA-314. *Phytochem. Lett.* **2019**, *32*, 1–5. [[CrossRef](#)]
19. Proksa, B. *Talaromyces flavus* and its metabolites. *Chem. Pap.* **2010**, *64*, 696–714. [[CrossRef](#)]
20. Nicoletti, R.; Trincone, A. Bioactive compounds produced by strains of *Penicillium* and *Talaromyces* of marine origin. *Mar. Drugs* **2016**, *14*, 37. [[CrossRef](#)]
21. Nicoletti, R.; Salvatore, M.M.; Andolfi, A. Secondary metabolites of mangrove-associated strains of *Talaromyces*. *Mar. Drugs* **2018**, *16*, 12. [[CrossRef](#)] [[PubMed](#)]
22. Yuan, W.H.; Teng, M.T.; Yun, Y.F.; Jiang, N.; Ma, L.; Sun, S.S.; Yuan, B.; Tang, J.; Wu, Q.Y.; Li, Q.; et al. Talarolactone A, an isocoumarin derivative fused with dihydrothiophene with selective antimigratory activity from the endolichenic fungus *Talaromyces* sp. *J. Nat. Prod.* **2020**, *83*, 1716–1720. [[CrossRef](#)] [[PubMed](#)]
23. Chen, S.H.; Liu, Y.Y.; Liu, Z.M.; Cai, R.L.; Lu, Y.J.; Huang, X.S.; She, Z.G. Isocoumarins and benzofurans from the mangrove endophytic fungus *Talaromyces amestolkiae* possess α -glucosidase inhibitory and antibacterial activities. *RSC Adv.* **2016**, *6*, 26412–26420. [[CrossRef](#)]
24. Buttachon, S.; May, Z.; War, W.; Dethoup, T.; Gales, L.; Pereira, J.A.; Silva, A.M.S.; Kijjoa, A. Secondary metabolites from the culture of the marine sponge-associated fungi *Talaromyces tratensis* and *Sporidesmium circinophorum*. *Planta Med.* **2016**, *82*, 888–896. [[CrossRef](#)] [[PubMed](#)]
25. Miao, F.; Yang, R.; Chen, D.D.; Wang, Y.; Qin, B.F.; Yang, X.J.; Zhou, L. Isolation, identification and antimicrobial activities of two secondary metabolites of *Talaromyces verruculosus*. *Molecules* **2012**, *17*, 14091–14098. [[CrossRef](#)]
26. Duo-Chuan, L.L.; Chen, S.; Jing, L.U. Purification and partial characterization of two chitinases from the mycoparasitic fungus *Talaromyces flavus*. *Mycopathologia* **2005**, *159*, 223–229. [[CrossRef](#)]
27. Bai, M.; Zheng, C.J.; Chen, G. Austins-type meroterpenoids from a mangrove-derived *Penicillium* sp. *J. Nat. Prod.* **2021**, *84*, 2104–2110. [[CrossRef](#)]
28. Bai, M.; Zheng, C.J.; Huang, G.L.; Mei, R.Q.; Wang, B.; Luo, Y.P.; Zheng, C.; Niu, Z.G.; Chen, G.Y. Bioactive meroterpenoids and isocoumarins from the mangrove-derived fungus *Penicillium* sp. TGM112. *J. Nat. Prod.* **2019**, *82*, 1155–1164. [[CrossRef](#)]
29. Liao, H.X.; Shao, T.M.; Mei, R.Q.; Huang, G.L.; Zhou, X.M.; Zheng, C.J.; Wang, C.Y. Bioactive secondary metabolites from the culture of the mangrove-derived fungus *Daldinia eschscholtzii* HJ004. *Mar. Drugs* **2019**, *17*, 710. [[CrossRef](#)]
30. Bai, M.; Zheng, C.J.; Nong, X.H.; Zhou, X.M.; Luo, Y.P.; Chen, G.Y. Four new insecticidal xanthene derivatives from the mangrove-derived fungus *Penicillium* sp. JY246. *Mar. Drugs* **2019**, *17*, 649. [[CrossRef](#)]
31. Bai, M.; Huang, G.L.; Mei, R.Q.; Wang, B.; Luo, Y.P.; Nong, X.H.; Chen, G.Y.; Zheng, C.J. Bioactive lactones from the mangrove-derived fungus *Penicillium* sp. TGM112. *Mar. Drugs* **2019**, *17*, 433. [[CrossRef](#)] [[PubMed](#)]
32. Liao, H.X.; Zheng, C.J.; Huang, G.L.; Mei, R.Q.; Nong, X.H.; Shao, T.M.; Chen, G.; Wang, C.Y. Bioactive polyketide derivatives from the mangrove-derived fungus *Daldinia eschscholtzii* HJ004. *J. Nat. Prod.* **2019**, *82*, 2211–2219. [[CrossRef](#)] [[PubMed](#)]
33. Zheng, C.J.; Bai, M.; Zhou, X.M.; Huang, G.L.; Shao, T.M.; Luo, Y.P.; Niu, Y.Y.; Chen, G.Y.; Han, C.R. Penicilindoles A-C, cytotoxic indole diterpenes from the mangrove-derived fungus *Eupenicillium* sp. HJ002. *J. Nat. Prod.* **2018**, *81*, 1045–1049. [[CrossRef](#)] [[PubMed](#)]
34. Yan, Z.Y.; Wen, S.; Ding, M.; Guo, H.X.; Huang, G.Y.; Zhu, X.T.; Huang, J.Y.; She, Z.G.; Long, Y.H. The purification, characterization, and biological activity of new polyketides from mangrove-derived endophytic fungus *Epicoccum nigrum* SCNU-F0002. *Mar. Drugs* **2019**, *17*, 414. [[CrossRef](#)]

35. Sun, J.; Zhu, Z.X.; Song, Y.L.; Ren, Y.; Dong, D.; Zheng, J.; Liu, T.; Zhao, Y.F.; Tu, P.F.; Li, J. Anti-neuroinflammatory constituents from the fungus *Penicillium purpurogenum* MHZ 111. *Nat. Prod. Res.* **2017**, *31*, 562–567. [[CrossRef](#)]
36. Qi, J.; Shao, C.L.; Li, Z.Y.; Gan, L.S.; Fu, X.M.; Bian, W.T.; Zhao, H.Y.; Wang, C.Y. Isocoumarin derivatives and benzofurans from a sponge-derived *Penicillium* sp. fungus. *J. Nat. Prod.* **2013**, *76*, 571–579. [[CrossRef](#)]
37. Li, S.D.; Wei, M.Y.; Chen, G.Y.; Lin, Y.C. Two new dihydroisocoumarins from the endophytic fungus *Aspergillus* sp. collected from the South China Sea. *Chem. Nat. Compd.* **2012**, *48*, 371–373. [[CrossRef](#)]
38. Zin, W.W.M.; Buttachon, S.; Dethoup, T.; Pereira, J.A.; Gales, L.; Inacio, A.; Costa, P.M.; Lee, M.; Sekeroglu, N.; Silva, A.M.S.; et al. Antibacterial and antibiofilm activities of the metabolites isolated from the culture of the mangrove-derived endophytic fungus *Eurotium chevalieri* KUFA 0006. *Phytochemistry* **2017**, *141*, 86–97. [[CrossRef](#)]
39. Arunpanichlert, J.; Rukachaisirikul, V.; Phongpaichit, S.; Supaphon, O.; Sakayaroj, J. Meroterpenoid, isocoumarin, and phenol derivatives from the seagrass-derived fungus *Pestalotiopsis* sp. PSU-ES194. *Tetrahedron* **2015**, *71*, 882–888. [[CrossRef](#)]
40. He, J.; Yang, M.S.; Wang, W.X.; Li, Z.H.; Elkhateeb, W.A.M.; Wen, T.C.; Ai, H.L.; Feng, T. Anti-phytopathogenic sesquiterpenoid-xanthone adducts from potato endophytic fungus *Bipolaris eleusines*. *RSC Adv.* **2019**, *9*, 128–131. [[CrossRef](#)]